Solid Earth Discuss., 6, 3141–3196, 2014
www.solid-earth-discuss.net/6/3141/2014/
doi:10.5194/sed-6-3141-2014

Solid Earth Discussions
Open Access

GrainSizeTools: a Python script for estimating the dynamically recrystallized grain size from grain sectional areas

M. A. Lopez-Sanchez and S. Llana-Fúnez

Departamento de Geología, Universidad de Oviedo, Spain

Received: 3 October 2014 – Accepted: 3 November 2014 – Published: 27 November 2014

Correspondence to: M. A. Lopez-Sanchez (malopez@geol.uniovi.es)

Published by Copernicus Publications on behalf of the European Geosciences Union.

Abstract

Paleopiezometry and paleowattometry studies, required to validate models of lithospheric deformation, are increasingly common in structural geology. These studies require a numeric parameter to characterize and compare the dynamically recrystallized grain size of natural mylonites with those obtained in rocks deformed under controlled conditions in the laboratory. We introduce a new tool, a script named *GrainSizeTools*, to obtain a single numeric value representative of the dynamically recrystallized grain size from the measurement of grain sectional areas (2-D data). For this, it is used an estimate of the most likely grain size of the grain size population, using an alternative tool to the classical histograms and bar plots: the peak of the Gaussian kernel density estimation. The results are comparable to those that can be obtained by other stereological software available, such as the *StripStar* and *CSDCorrections*, but with the advantage that the script is specifically developed to produce a single and reproducible value avoiding manual steps in the estimation, which penalizes reproducibility.

1 Introduction

Dynamic recrystallization was defined by Stunitz (1998) as "the reconstruction of crystalline material without a change in chemical composition driven by strain energy in the form of dislocations". Two mechanism of dynamic recrystallization have been identified (see a review in Urai et al., 1986 and references therein): (1) grain boundary migration (Poirier and Guillopé, 1979) and (2) progressive subgrain rotation (Poirier and Nicolas, 1975). The activation of these recrystallization mechanism depend on several factors, such as temperature, pressure, strain rate, presence of fluids, etc., and the interaction between these mechanism, to a greater or lesser degree, produces three easily identifiable types of dynamic recrystallization microstructures: (1) bulging recrystallization (or BLG), (2) subgrain rotation (or SGR); and (3) grain boundary migration (or GBM) (see Stipp et al., 2002 for details). The determination of the recrystallized grain size

SED
6, 3141–3196, 2014

distribution in a deformed polycrystalline aggregate is one of the increasingly common tasks in structural geology and tectonics that study crystal plastic deformation in rocks at the microscale. Although there is no universally accepted model to explain the relationship between dynamically recrystallized grain size and deformation conditions (see De Bresser et al., 2001; Austin and Evans, 2007; Shimizu, 2008; Platt and Behr, 2011), it is clear that the dynamically recrystallized grain size is a key variable to determine the mechanical properties of dynamically recrystallized rocks. Experimental studies have demonstrated that dynamically recrystallized rocks evolve to a stable dynamically recrystallized grain size value during deformation by dislocation creep (Means, 1983; Pieri et al., 2001; Barnhoorn et al., 2004; Stipp et al., 2006). These steady-state dynamically recrystallized grain size have also been inferred in natural mylonites (e.g. Michibayashi, 1993; Herwegh et al., 2005). However, it is not well known whether this stable dynamically recrystallized grain size is represented by a single value of grain size or, most probably, by a stable continuous range of grain sizes with a particular distribution (normal, log-normal or others) and properties.

The observations outlined above led some authors to relate the dynamically recrystallized grain size (D) with the magnitude of the applied stress (i.e. the flow stress) with a relation of the type $D = A\sigma^{-m}$, where A and m are material and mechanism-specific constants (Luton and Sellars, 1969; Nicolas and Poirier, 1976; Twiss, 1977; Gillopé and Poirier, 1979; Ross et al., 1980; Schmid et al., 1980; Rutter, 1995; Stipp and Tullis, 2003) or with the rate of mechanical work (Austin and Evans, 2007); in other words, to use the dynamically recrystallized grain size as a paleopiezometer or paleowattometer respectively. Since there are no measures so far taken in situ within the lower crust or the lithospheric mantle (see Kozlovsky, 1987; Emmermann and Lauterjung, 1997 for the current limits reached so far), the paleopiezometry and paleowattometry studies in ancient exhumed mylonitic rocks are the key to constrain the theoretical strength profiles estimated for the lower crust and the lithospheric mantle, and therefore, to validate the models of lithospheric deformation.

SED
6, 3141–3196, 2014

Paleopiezometry and paleowattometer methods are based on constitutive flow laws calibrated by rock deformation experiments. In these studies several parameters are controlled and others monitored during the deformation experiment. Once a mechanical steady-state is achieved (or assumed in the case of asymmetric shortening) and the experiment interrupted and quenched, the grain size of the polycrystalline aggregates deformed during the experiment can be measured in specific areas of the deformed specimen. In order to apply correctly rheological laws in naturally deformed rocks, the methodology used to estimate the dynamically recrystallized grain size in experimentally deformed specimens and naturally deformed rocks should correspond so that reproducible results can be obtained (see for example Stipp et al., 2010). Unfortunately, this simple step is seldom followed, mainly due to the use of different parameters to characterize the size of a grain (e.g. the average diameter, the maximum length, etc.) and in part due to the various available methods to estimate the actual dynamically recrystallized grain size from thin sections (see Higgins, 2006; Berger et al., 2011).

Briefly, the methods for measuring grain size can be separated into three groups (Berger et al., 2011): (i) 1-D data (i.e. line intercept methods, number of grains per unit area or grain boundary density), (ii) 2-D data (based on the estimation of the grain sectional areas using image analysis tools); and (iii) 3-D methods (computed tomography, serial sectioning). 3-D methods are the best since we are dealing with real volumes. However, 3-D methods are still far from being a common technique due to being time-consuming, costly and in some cases not lacking technical limitations. In fact 3-D methods are not always applicable, especially in dynamically recrystallized mylonites in which most of the grains in contact are of the same phase. 1-D methods, especially the line intercept method, are the most widely used analysis technique used to measure dynamically recrystallized grain size in monophase deformed rocks in the literature (e.g. Abrams, 1971; Karato, 1980; Rutter, 1995; Post and Tullis, 1999). However, these 1-D methods only report one value (1-D), the average grain size, without considering the distribution of the population or apply stereological corrections and, therefore, suffer from several limitations (Heilbronner and Brun, 1998; Higgins, 2000,

SED
6, 3141–3196, 2014

2006; Berger et al., 2011). Another severe limitation is that 1-D methods only apply in case of monomineralic aggregates or samples (at thin-section scale). Nowadays, the more efficient way to estimate the dynamically recrystallized grain size is therefore the use of 2-D methods (see Heilbronner and Brun, 1998; Berger et al., 2011). 2-D methods imply the measurement of the individual parameters (usually sectional areas but also others) of each grain from a thin section using image analysis. To perform this task, there are several public-domain open-source cross-platform image-processing programs available, such as *ImageJ* (Scheider et al., 2012). With this software, we obtain the full – or almost full due to optical limitations – distribution of diameters and other microstructural descriptive parameters of grains within the aggregate (Heilbronner and Brun, 1998; Heilbronner, 2000; Herwegh, 2000; Berger et al., 2011). This standard approach also has well-known limitations since it requires the assumption that all crystals have the same simple shape. In fact, in cases where the objects are geometrically more complex than a sphere there is commonly a non-unique solution to the distribution of measured grain sizes (Higgins, 2000, 2006).

As previously mentioned, it is expected that highly deformed recrystallized rocks, such as mylonites with a complete or quasi-complete dynamic recrystallization microstructure, reach a stable dynamically recrystallized grain size for the mineral phase under consideration under constant deformation conditions. In other words, the microstructure during deformation reaches some sort of steady-state. Furthermore, in some cases it is assumed that the shapes of the recrystallized grains are similar or close to a sphere (near-equant objects). This assumption seems acceptable most of the time for some of the most common dynamically recrystallized non-tabular grains in crustal and mantle shear zones such as olivine, quartz, feldspar and calcite, at least when the main mechanism of dynamic recrystallization is not "fast" grain boundary migration (GBM), which produces lobate-shaped grains. This means that when studying dynamically recrystallized olivine, quartz, feldspar and calcite mylonites it is expected that in most of the cases we are dealing with the following scenario: (1) a steady-state dynamically recrystallized grain size (with a unique value or a continuous range with

SED
6, 3141–3196, 2014

a particular distribution of grain sizes) and (2) grain shapes close or not too far from the simplest shape (i.e. sphere). Under such circumstances, there are several advantages to estimate the actual dynamically recrystallized grain size from a thin section (see Royet, 1991; Higgins, 2000).

In this work, we first review the available methods used to estimate the grain size from two-dimensional area section data and establish a set of instructions as robust as possible leading to a single numeric value that represents the dynamically recrystallized grain size. The second aim is to write a script implementing this protocol, checking that it provides reliable and reproducible results. Although there is free software available to estimate the dynamically recrystallized grain size based on 2-D approach and stereological considerations, such as *StripStar* (Heilbronner and Brun, 1998) or *CSD-Corrections* (Higgins, 2000), they are not open source and cross-platform (e.g. *CSD-Corrections*), they require many steps and the use of more than one software package to obtain the final results (e.g. *StripStar*), and, most important, they are not specifically designed to generate a single numeric value from the grain population under study. Our goal is to create a script meeting the following criteria: (i) it is written in a free and easy to read programming language that runs on all different platforms (Windows, Mac OS X, Linux, Unix), (ii) the use of the script does not require any knowledge of programming to use (i.e. user-friendly), (iii) provide a free and open source code organized in a modular way making it easier to modify, reuse or extend by anyone with programming skills if necessary; and (iv) the script must produce by itself the result required and and ready-to-publish figures (i.e. there is no need of other software to produce figures or further treatment of data).

2 Grain size from sectional grain areas in ideal monodisperse distributions

To obtain a grain size value from a thin-section it is necessary to choose a correct parameter to describe the two-dimensional size of the grains. There are several parameters, such as the feret maximum length, the ellipse major of minor axis, etc. (see Hig-

SED
6, 3141–3196, 2014

gins, 2006; Heibronner and Barret, 2014). When particles are expected to be spherical or close to a spherical shape (near-equant objects), its 3-D size can be uniquely characterized by their diameter (or the average diameter if they are not perfect spheres). In this case, we think the best way to proceed is to convert the cross-sectional areas of each individual grain into an individual 1-D length, the diameter (d) of the grain, via the equivalent circular diameter (Heilbronner and Brun, 1998; Herwegh, 2000; Berger et al., 2011):

$$d = 2\sqrt{\frac{\text{area}}{\pi}} \tag{1}$$

Now consider the simplest grain size distribution in which all grains have similar shape (i.e. spheres) and size, this is called a monodisperse distribution. When a monodisperse system of grains is cut randomly, as in a thin section, the cut-section effect occurs, i.e. the intersection plane rarely cuts exactly through the centre of each grain (our pseudo-spherical particles) (Fig. 1). Therefore, the diameters obtained from the sectional areas are a population of apparent diameters that can theoretically vary between zero and the actual diameter of the grains (Fig. 1). In perfect monodisperse populations, the maximum diameter obtained from the data set would be the closest to the actual diameter and the accuracy of the grain size estimation only depends on choosing an appropriate sample size for the accuracy we are looking for (see Appendix A for details). Unfortunately, and leaving aside that most if not all natural mylonites show a continuous dynamically recrystallized grain size range instead of a unique grain size, this is an oversimplification and in dynamically recrystallized samples it is not trivial in many cases to distinguish sections of true recrystallized grains from those which are not or, in some cases, to distinguish a grain boundary from a sub-grain wall. This means that it is common to include within the data set grains with sizes (apparent diameters) larger than the actual recrystallized grain size. The inadvertent introduction of outliers can produce unreliable results in the estimate if we consider only the maximum value.

SED
6, 3141–3196, 2014

An alternative approach is to look at the distribution of apparent diameters obtained when set of randomly distributed spherical grains is cut through and derive a parameter that describes the grain size from the whole population of apparent diameters. We can implement a Monte Carlo simulation to generate monodisperse and more complex populations of spherical grains randomly cut (see Appendix B) and observe the properties of the distribution of the apparent diameters obtained. Although there are several ways to represent this type of data (see Higgins, 2006), we will focus only on two of the most typical: representing the numerical density distribution of apparent diameters obtained in a histogram plot, known as the number weighted plot, or, the less common way, representing the area percentages of equivalent diameters in a bar plot (i.e. the sum of the areas of the grains respect to the total for each grain size interval defined), known as the area-weighted plot (Herwegh, 2000; Berger et al., 2011).

As noted in Fig. 2a, the probability of cutting sections through a circle at different size intervals is not equal and therefore do not produce a uniform distribution but a unimodal one. The histograms shown in Fig. 2a reveal some remarkable features. First, the probability of cutting sections with lengths close to the actual diameter is always higher. These theoretical distributions show an extreme case of negative skew (also known as *J-shape* distribution) due to the ceiling effect, this is, the data point cannot rise above a certain value, in this case the actual diameter (Fig. 2a). As a simple example, the probability of obtaining apparent diameters larger than the half of the actual diameter is $P = 0.87$ (Fig. 1b). As expected, if a smaller bin size is selected (Fig. 2a), the actual diameter of the grain population are always within the most frequent class (interval) of the histogram: the modal interval. It is also remarkable that there is a significant difference between the interval with the maximum frequency and the next closest, even in the case we choose a considerable number of classes (Fig. 2b). This means that it is very easy to find the modal interval in a histogram plot, even graphically. This approach also has clear advantages when compared to the previous method in the case that outliers are present in the collection of grains, because it is not expected that the outliers produce higher frequencies within the histogram due to their random nature

SED
6, 3141–3196, 2014

(as long as the bin size/width established is not too large to produce misleading results) (see later). The modal interval is one of the statistical parameters commonly used to characterize the dynamically recrystallized grain size from population of apparent diameters but also from the derived 3-D grain size distributions (e.g. Berger et al., 2011). The other statistical parameter commonly used to characterize the dynamically recrystallized grain size is the mean of the population, although the median was also used (see Ranalli, 1984). As can be seen in Fig. 2, if the population size is representative of the sample, the actual diameter is 1.28 times the mean of the entire apparent diameter population (or the mean 0.79 times the actual diameter). This is the reason why the mean dynamically recrystallized grain size obtained with 1-D methods is sometimes multiplied by a factor (or constant) to estimate the actual size. As discussed later this approach is not optimal to reach reproducibility when outliers exist and can lead to large errors in estimating the actual dynamically recrystallized grain size. In the case of the area-weighted diagrams (Fig. 2b) the distribution show similar features, although as expected, the frequency of the apparent diameter intervals close to the actual grain size is more pronounced than in the number weighted approach. Another remarkable difference is that the area-weighted mean grain size is closer to the actual grain size (specifically 0.96 times) than the mean grain size. The area-weighted mean grain size has the same limitations as the use of the mean grain size.

It is important to highlight that the estimation of the modal interval compared to the mean or the area-weighted mean has the constrains inherent to the use of histograms and bar plots: (1) it is necessary to define the same left edge of the bin and the same bin size/width (or number of classes) to yield reproducible results in similar populations, and (2) they are not smooth. To use this approach (i.e. find the most likely dynamically recrystallized grain size of the distribution) over the mean or the area-weighted mean, it would be useful to overcome these constrains. The issue of the left edge of the bin is easy to solve. Although in practice the actual left edge of the bin is set by the optical and image resolution limitations of the technique applied (Higgins, 2006), which means that it can vary across different studies, we know that the actual theoretical left edge of the

SED
6, 3141–3196, 2014

bin is zero and we can set this limit at zero to improve reproducibility. The problem with the discrete nature of histograms and bar plots is inherent to the technique, and means that we obtain a modal interval instead of a single value, while at the same time the size of the interval depends on the bin size chosen. To convert this interval into a single value we have to choose which value within the interval is the best. Some software's (e.g. *CSDCorrections*) used the middle value, but as shown in Fig. 3 it is impossible to know whether the actual diameter corresponds to the upper limit of the modal interval (as in examples of Fig. 2a and b), any other value within the modal interval or even within the modal interval, since in real cases we do not know the actual dynamically recrystallized grain size we are looking for and therefore do not know if the selected bin size is a perfect multiple of the same.

The other critical factor to consider is the bin size/width. This parameter is directly related with the precision of the grain size estimation since it is assumed that the actual dynamically recrystallized grain size is within the modal interval obtained or close to the same (Fig. 3). If large bin sizes are selected, a gain or a loss of accuracy can occur but always at the cost of precision. On the other hand, if a small bin size is selected, then misleading results are more likely (e.g. the bin size must not exceed the measurement uncertainty in data). To yield producible results it would be necessary to implement an automatic process – an algorithm – that sets an optimal bin size based on the features of the population under study.

3 The Gaussian kernel density estimator as an alternative to the histogram

To overcome some of the inherent problems in the use of histograms we can use an alternative approach in the case of the number weighted approach: the Gaussian kernel density estimator or Gaussian kde. The Gaussian kde is, as the histogram, a non-parametric density estimator but it is smooth and independent of end points (Fig. 4). The interpretation of the data distribution still depends on the bandwidth chosen (the equivalent to the histogram's bin size/width), which strongly influences the shape of the

SED
6, 3141–3196, 2014

Gaussian kde and, therefore, the location of the peak value. It is therefore necessary to implement a reliable method to perform this task. In any event, there are plenty of methods to find the optimal kernel bandwidth in literature depending on the expected features of the data set (see Scott, 1992; Turlach, 1993; Bashtannyk and Hyndman, 2001). The use of the Gaussian kde also has the advantage that it does not provide an interval, as in the case of using histograms, but a unique value (the peak value) that represents the most probable value of dynamically recrystallized grain size in a population of grains (see examples in Fig. 2c and e). This prevents having to choose which one is the most representative value of the actual dynamically recrystallized grain size within the modal interval, which as shown in Fig. 3 is impossible to know.

In summary, the assumptions and key features of the model to find the actual recrystallized grain size from 2-D data (sectional areas) and to implement within the script are:

- All dynamically recrystallized grains are near-equant objects approaching spherical shape. The grains can therefore be characterized solely by their diameter (or average diameter) using the equivalent circular diameter from their areas.
- There will be outliers and some measurement errors within the data set.
- Dynamic recrystallization results in a stable grain size – a steady-state microstructure – for a particular mineral phase. The stable recrystallized grain size can be represented by a single value: the actual grain size in case of monodisperse distributions and the most likely grain size in case of continuous grain size distributions. It is assumed that in the case of "equilibrium", a continuous grain size distributions would fit a log-normal distribution (see later).
- The Gaussian kernel density estimator is a useful non-parametric tool and has several advantages compared to histograms.

SED
6, 3141–3196, 2014

4 The GrainSizeTools script

The script is written in Python, a general-purpose high-level interpreted programming language characterized by a clear syntax and ease of learning. The main advantages of Python language are: (i) it is free and open-source, (ii) the underlying computer language run on all different platforms (Windows, Mac OS X, Linux or Unix), (iii) there are a large number of open and freely available scientific libraries providing an interactive environment for algorithm development, data analysis, data visualization and numeric computation; and (iv) due to the preceding points, particularly the last one, the use of Python is becoming increasingly popular in academia and in science in general.

The *GrainSizeTools* script can be downloaded from https://sourceforge.net/projects/grainsizetools/ and requires the three following scientific Python libraries: Numpy, Scipy (Oliphant, 2007) for data analysis, and MatplotLib (Hunter, 2007) for plotting. The script produces several types of output, allowing to save the graphical output as bitmap (8 file types to choose) or vector images (5 file types to choose). Although the script is designed to produce figures ready for publication, they can be easily customise within the MatplotLib environment (i.e. when the figure is showed by the script and prior to save it as a file) or by post-editing the vector image in vector-graphics applications such as Adobe Illustrator, ACDSee Canvas, Inkscape or similar. Another important point is that to use the script there is no need for prior knowledge of the Python language. The steps to estimate the recrystallized grain size are easy to achieve and a quick tutorial can be found online (http://sourceforge.net/p/grainsizetools/wiki/Home/).

4.1 A brief description of the script

The script is organized in a modular way using Python functions. This facilitates to modify, reuse or extend the code and allows specifications of each function. In the specifications, the user will find the assumptions made, the conditions that must be met for the inputs and the result/s obtained for each one.

SED
6, 3141–3196, 2014

The script can be divided into three main parts or functions with intuitive and self-explanatory names:

The first part is a function called “importdata” responsible for loading the data set into memory for subsequent manipulations. The data has to be previously stored in a text file such as txt (a data on each line) or csv (comma-separated values). This file is previously created with the image analysis software used to measure the sectional areas of the grains.

The second part is a function called “CalcDiameters” that returns an array of the diameters calculated from the sectional areas assuming that the grains are near-equant objects. In the event that the grains slightly depart from near-equant objects, the value would represent the diameter of a sphere of equivalent volume. If applicable, it also allows to correct the diameters calculated by adding the perimeter of the grains not previously included in the image analysis.

The third part is a function called “findGrainSize” that returns the number and area-weighted plots, the location of the Gaussian kernel density estimator peak, the modal intervals and their middle values produced by both approaches and other relevant information such as the bin size and the Gaussian kde bandwidth estimated.

The protocol in the script to do this is explained below:

As portrayed above and shown in Fig. 3, choosing a different bin size (or number of classes) could lead to a different interpretation of the data distribution and, therefore, different results. To ensure reproducibility, the idea behind the script is that for similar populations similar bin sizes need to be used. For this, the idea is to avoid as far as possible manual data manipulation steps and use an automated process, this is, to find an algorithm that estimates on its own the optimal bin size. Although there is no best number of bins, there are some guidelines or rules of thumb to determine the optimal number of bins. *GrainSizeTools* implements two of the most commonly used rules of thumb to find the optimal number of bins: the Scott rule (Scott, 1979) – based on the sample SD – and the Freedman–Diaconis rule (Freedman and Diaconis, 1981) – based on the sample interquartile range. The rule used by default within the script

SED
6, 3141–3196, 2014

is the Freedman–Diaconis rule since it is less prone to outliers in comparison to Scott rule. In principle, it is unreasonable that the bin size exceeds the uncertainty of the data acquired during the calculation of apparent diameters from the measured grain areas, around 4 % according to Berger et al. (2011). Because the actual diameter of the grains is unknown when we applied for the first time "findGrainSize" function, it is impossible to know if the bin size estimated is lower than the 4 % error limit. For this, the user can set later, if necessary, a larger user-defined bin size based on the assumed error during data acquisition and the actual dynamically recrystallized grain size estimation obtained in the first try. The same rules applies for the area-weighted approach, based on Herwegh (2000), that uses the sum of the areas respect to the total area (area percentages) of cross-sectional shapes for each grain size interval defined. This allows the comparison between distributions in number and area-weighted plots in order to obtain complementary information about the data set. The script returns the modal intervals and the middle values of the modal intervals in both cases. It also returns the area-weighted mean of the data set.

The script also implements the Gaussian kernel density estimator within the number weighted plot. It finds and returns the peak value of the kde function; this is, the most likely value of dynamically recrystallized grain size according to the number weighted approach. To estimate the optimal bandwidth of the Gaussian kde we use the Silverman rule of thumb method (Silverman, 1986), since such method works well for univariate systems with unimodal densities (Turlach, 1993; Bashtannyk and Hyndman, 2001). The implementation also allows to use the Silverman rule multiplied by a constant to modify the bandwidth for comparative purposes.

5 Testing the mean, the modal intervals and the Gaussian kde peak

Ideal monodisperse grain populations, such as described in Sect. 2, do not exist in natural or experimentally deformed samples. In fact, in grain size studies of dynamically recrystallized mylonites it is extremely uncommon – if they exist – to observe

SED
6, 3141–3196, 2014

perfect *J-shaped* distributions of apparent sizes. This is due to the presence of outliers and different errors introduced during data acquisition, but mainly because most recrystallized mylonites show a continuous range of dynamically recrystallized grain size instead of a single grain size. Our aim is to test the different parameters obtained by the script against the introduction of outliers, errors, and more complex populations of grains, as multimodal populations or populations with a continuous distribution of dynamically recrystallized grain size. For clarity, we first focus on the modifications induced by the presence of outliers and different sources of errors in the mean, the area-weighted mean, the modal intervals and the Gaussian kde peak in monodisperse systems. Then, we will focus on populations with different dynamically recrystallized grain sizes (i.e. polydisperse).

5.1 Sources of errors

Figure 5a and b illustrates a situation in which 20 % of the data are outliers which were randomly introduced in a monodisperse population apparent section of grains. Larger grains correspond to sections of grains that have not been fully recrystallized (see Appendix B for details). As expected, the mean and the area-weighted mean are affected by the introduction of these outliers shifting the expected values to higher values. Another non-negligible source of error arises when the smallest grain sizes are not measured due to optical and image resolution limitations of the technique applied (Higgins, 2006; Berger et al., 2011). This means that in the real distributions the smallest values tend to reflect the optical or resolution limitations of the applied technique instead of tending to zero as they would in theory. This effect also tends to slightly shift the mean and the area-weighted mean to higher values (Fig. 5c and d). It is noteworthy that the modal intervals and the Gaussian kde peak in these cases are not affected by these errors provided that the bin size and/or the bandwidth chosen are the same (in case of histograms and bar plots also the left edge of the bin) (Fig. 5). Figure 5c and d shows another non-negligible feature in real samples: the effect of uncertainty in grain measurement in the distribution of apparent diameters. In this case, the presence of

SED
6, 3141–3196, 2014

grain sizes above the actual diameter of recrystallized grains modify the ideal *J-shape* distribution, although it does not affect the parameters mentioned above if the population is representative. It is important to note that the examples portrayed here are just specific situations and, in fact, combinations of different sources of errors in the determination of dynamically recrystallized grain size in natural samples are expected, particularly when the delineation of grains is an automated process.

To sum up, the variations in the estimate of the mean and the area-weighted mean showed in Fig. 5 are proof that these parameters are not reliable when the presence of outliers is significant. This also precludes the use of multiplying the mean by a constant to obtain an approximation of the actual dynamically recrystallized grain size in monodisperse systems since the nature of the errors is random. On the other hand, the modal interval and the Gaussian kde peak are less prone to errors introduced by outliers and by the limitations of optical resolution compared to the mean.

5.2 Testing the mean, the modal intervals and the Gaussian kde peak in synthetic polydisperse samples

In our case, polydisperse systems refer to recrystallized grains with the same spherical or near-equant shape but with different discrete values of grain size or a continuous range of grain size (unimodal or multimodal) instead of a discrete value. For simplicity, we will consider separately an example of populations with two or more different discrete grain sizes (bimodal or multimodal discrete distributions) and examples with a unimodal continuous grain size range. Based on previous studies, the most common situation in dynamically recrystallized rocks in nature and experiment is that the microstructure reaches some sort of steady-state, which translates into a continuous range of dynamically recrystallized grain size instead of a unique value. With respect to the latter, although it is no clear what type of continuous distribution best describes this "equilibrium" dynamically recrystallized grain size, we have considered based on previous experience one of the most common continuous distributions in nature: the log-normal distribution, in this case with base e (i.e. the natural logarithm). In the case

SED
6, 3141–3196, 2014

of multimodal grain size distributions we will consider for simplicity a system with more than one discrete value of grain size. On the other hand, in the system with a continuous range of grain size we will consider unimodal systems.

Polydisperse populations of spheres/grains show, as a consequence of the mixture of sizes, another geometric effect to be considered beside the cut-section effect named the intersection-probability effect (Higgins, 2000). This refers to smaller grains being less likely to be intersected by a plane (i.e. the thin section) than larger ones. Hence, this effect needs to be accounted for in the simulation of polydisperse populations of dynamically recrystallized grain sizes (see Appendix B for details).

5.2.1 Bimodal (and multimodal) grain size distributions

Bimodal distributions are typical of two-phase mylonites in which the two phases reach under similar deformation conditions a different dynamically recrystallized steady-state grain size. The best approach is to deal with them separately (see examples in Herwegh, 2000; Heilbronner and Bruhn, 1998), although as we shall see it is no easy in all the cases and it is also useful to represent the area-weighted plot of the two mineral phases within the same plot (Fig. 6). A bimodal distribution can also be caused in monophasic mylonites by issues of choosing a wrong scale of study. As an example, we could be measuring several thin sections of the same shear zone that show dynamically recrystallized grain size changes at decametric scale. Another example of bimodal distribution in monomineralic samples at hand-specimen scale have been reported in experimentally deformed Carrara marble samples at large strains ($\gamma = 29$ and $\gamma = 50$) and high temperature (Barnhoorn et al., 2004), or in quartzitic mylonites with different slip systems operating simultaneously, in which quartz grains with *c* axis close to *Y* axis (prims) were larger than others with a different crystallographic orientation (Knipe and Law, 1987; Mancktelow, 1897; Heilbronner and Tullis, 2006). In monomineralic samples is much more difficult to separate dynamically recrystallized grain size populations; although in the latter case this could be done if we have a lattice preferred orientation map of the sample.

SED
6, 3141–3196, 2014

As shown in Fig. 6, in bimodal (or multimodal) cases the weighted area approach allows the user to know which of the two populations of grain size represents the predominant phase in volume (i.e. the volumetric contribution), which matters for rheology considerations (Herwegh, 2000; Berger et al., 2011). This is because the number weighted approach tend to place the modal interval in the population of smaller grain size even when it is not the main phase, especially when the difference in grain size between the two populations is small (Fig. 5a and b). As expected, the mean values in these cases produce meaningless results. In contrast, the modal intervals (i.e. the local maximums) or the local Gaussian kde peaks reflect the actual size (or the theoretical most common size in case of a two or more continuous grain size distributions) of different grain populations.

As in a previous example (see Fig. 5a), Fig. 6a shows that in systems with discrete values of grain size (uni- or multimodal) the Silverman rule tends to smooth excessively the population of apparent diameters of grains. We found – based on empiricism – that the Silverman rule multiplied by 1/3 yields best estimates (i.e. best accuracy) in these cases.

5.2.2 Log-normal dynamically recrystallized grain size distributions

Skewed distributions are particularly common in nature and often continuous distributions closely fit a log-normal distribution (Limpert et al., 2001). As an example, grain size ranges in sediments or non-deformed igneous rocks are typically log-normally distributed. It is rather common in dynamically recrystallized rocks that the 2-D or the derived 3-D dynamically recrystallized grain size distribution plots show long tailing distributions skewed to the right (see examples in Heilbronner and Bruhn, 1998; Heilbronner and Tullis, 2006; Berger et al., 2011; Heilbronner and Barret, 2014), which fits with the typical properties of this type of distribution. Based on these examples, it seems that at least some dynamic recrystallized mylonites reach a log-normal distribution of dynamically recrystallized grain size for a specific mineral phase (e.g. Ranalli, 1984; Michibayashi, 1993).

SED
6, 3141–3196, 2014

A random variable x – in our case x is the diameter of the grain – is said to be log-normally distributed if $\log(x)$ is normally distributed (Fig. 7). Continuous log-normal distributions have two features, only positive values are possible for the variable and the distribution using a linear scale is skewed to the right (Fig. 7). Although log-normal distributions can be characterized by different parameters, we will use the scale (denoted as μ^*) and shape (denoted as σ^* or s^*) since they describe the data directly at their original linear scale (Limpert et al., 2001). As noted in Fig. 7 they correspond with the "back-transformed" values of mean (μ) and SD (σ) of the $\log(x)$ distribution and they are referred as the geometric mean or median (μ^*) and the multiplicative SD (s^*) respectively (Limpert et al., 2001). The multiplicative SD (s^*) controls the shape of the log-normal distribution (Fig. 8). Thus, if s^* takes a value of 1 we obtain a normal (Gaussian) distribution. However, if it takes much larger values, the shape of the log-normal distributions becomes increasingly skewed to the right (Fig. 8). In general most s^* values measured in nature range from 1.4 to 3 (Limpert et al., 2001).

To test the Gaussian kde peak estimator with log-normal dynamically recrystallized grain size populations it is necessary to simulate a set of random different log-normal populations. Because there are no previous studies showing the typical features of continuous log-normal distribution of grains in recrystallized mylonites, we need to assume, based on the dynamically recrystallized grain size plots appearance in previous studies, a range of shape and scale parameters to simulate a finite number of log-normal distributions. With this in mind, the shape parameter in recrystallized mylonites probably ranges between 1.3 and 2.0 (cfr. Fig. 8 with previous dynamically recrystallized grain size studies in mylonites). To set a range of scales the same principle applies. Hence different scale values (up to 38) will be tested to obtain a range that yields a reasonable set of representative log-normal distributions of dynamically recrystallized grain size. With these constrains, we randomly generate populations of spherical grains with different values of mode (i.e. the grain size value we are looking for), shape and scale. Then, the cut-section and the intersection-probability effects are applied to the actual population to simulate a 2-D distribution of apparent diameters, and finally

SED
6, 3141–3196, 2014

the Gaussian kde peak location is calculated. One hundred trials were generated in each simulation with pre-defined features. Ultimately, different statistical parameters are calculated to see how the parameters affect the estimations. It was also checked how a modification of the Silverman rule bandwidth estimator affects the Gaussian kde peak estimations.

The results obtained indicate that the behaviour of the Gaussian kde peak estimator is complex since it depends, to a greater or lesser extent, on the three variables considered (Fig. 9). Firstly, the estimations can be slightly over- or underestimate the actual value of the most probable grain size, although always with a theoretically reasonable accuracy. The precision and hence the reproducibility of the estimations – which is the key in this study – also depends on the considered variables. We observe that the higher the scale and the smaller the grain size the lower is the precision (Fig. 9a and b). Something similar occurs with the shape parameter although the changes are not as noticeable (Fig. 9c). The highest 2-sigma absolute error obtained for the Gaussian kde peak in all simulations performed was ±2 (±5.4 % in relative error). Most of simulations yield relative 2-sigma errors below ±4 %, so theoretically the Gaussian kde peak estimator seems a robust estimator. However, the simulations performed warn that in case of a continuous log-normal population of dynamically recrystallized grain sizes in which the most probable dynamically recrystallized grain size is small (say smaller than 30 microns) and with a large range of dynamically recrystallized grain size (say higher than 100 microns), special care should be taken using the Gaussian kde peak estimator. In this case it would be desirable to use more than one parameter, such as the mean or the area-weighted mean, to compare between mylonites. Lastly, in the cases tested the modified version of the Silverman rule used in discrete models (the rule multiplied by 1/3) yielded worse accuracy and precision.

Although it is likely that real dynamically recrystallized grain size populations in mylonites are within the limits of the cases tested, it is unknown – because of the lack of previous studies on this matter – whether the scales and shapes considered are realistic in some, or maybe in most, cases. Consequently we think the best way to

SED
6, 3141–3196, 2014

test the reliability of the Gaussian kde estimator against other parameters is using real samples and compare it with the other parameters available (see Sect. 7 below). While the simulations performed have a lot of limitations due to all the assumptions made and the error data obtained have to be carefully considered, these simulations yield useful information since they allow us to understand how different parameters of the population affect the estimation.

6 How many grains are needed to achieve reproducibility?

Before to proceed and test the script in natural samples and against other software available, it is necessary to deal with the issue of how many grains are needed to achieve reproducibility. This is a non-trivial question as for comparison of different studies it is a necessary condition to have reproducibility. Previous studies state that more than 500 grains are necessary (Heilbronner and Bruhn, 1998; Heilbronner, 2000) or a number of 200–250 grains (Berger et al., 2011) for dynamically recrystallized grain size analysis. Since these studies did not explicitly address how they estimated the minimum number of grains needed for dynamically recrystallized grain size analysis, we assume these numbers rely solely on practical experience and are not derived by some theoretical underlying principle. With the aim of solving this issue and as a first approach, we have implemented a Monte Carlo simulation to determine the minimum necessary sample size from a theoretical point of view in the case of monodisperse population of grains (see Appendix C). In this case, the given condition is based on the typical uncertainty of measurements. Berger et al. (2011) found that when repeating the measurement in the same targeted grain the error margins in the diameters calculated ranged between 1 and 4 %. Taking the 4 % error margin, our goal is to find the minimum number of grains needed so that if the measurement are repeated a number of times, nearly 95 % (2-sigma) or 99 % (3-sigma) of the time the mean calculated shows a variation equal or less than 4 %. In other words, the error that is obtained due to technical limitations when we estimate the apparent diameters from the images

SED
6, 3141–3196, 2014

(~ 4 % for targeted grains) is larger than the error obtained when the statistical methods to obtain a value representative of the grain size 3-D population from the 2-D data are applied.

As can be deduced from the plots showed in Fig. 10, this condition is satisfied for monodisperse populations of spheres when the number of measured grains is 203 in the case of sigma-2 or is 455 grains in the case of sigma-3. These values were calculated assuming a perfectly monodisperse population of grains. This means that due to different sources of error and that the common event of reaching a continuous range of grain size instead of a unique value in real samples, the minimum sample size should be always higher than those shown here.

To set a more reliable minimum number of grains needed to achieve reproducibility it is necessary to use the same criteria applied in the previous simulation but using grain populations with a continuous range of dynamically recrystallized grain size. However, due to the infinite number of possible continuous distributions to consider the task seems impossible to accomplish, at least until we have a reliable knowledge about the type and parameters that characterize the dynamically recrystallized grain size continuous distributions in real mylonites. To overcome this situation, a large data set of natural dynamically recrystallized deformed rock can be used. The strategy – known as bootstrapping – is to perform a random resampling of the data set chosen and see how the sample size affects the results of the parameters that characterize the population of dynamically recrystallized grain sizes by comparing this to the results obtained using the whole population. For this, we use a population of dynamically recrystallized quartz grains measured in a natural deformed granite, sample MAL-05 (see below for details; Sect. 7) with a population of 2945 grains. It is assumed that this large number of grains contains all the information necessary to fully characterize the recrystallized grain size.

Following the same principle as in the above Monte Carlo simulation (see Appendix C for details), we found that the mean obtained from a large number of random samples has an error less than 4 % when the sample size is 428 for sigma-2 (~ 95 % of the time) or 954 for sigma-3 (~ 99 % of the time) (Fig. 10). It needs to be taken into account that

SED
6, 3141–3196, 2014

if anyone performs the same simulation they would probably obtain slightly different results. The reason for this is that the coefficient of variation line is nearly parallel to the x axis when approximate to the value of 4 % and have an arbitrary noise due to the stochastic nature of the simulation (see the inset in Fig. 10d). This produces a range of values instead of a unique value. To overcome this, we performed ten simulations and with the results obtained it was estimated the Bayesian credible intervals (i.e. the true value falls within the credible region 95 % of the time), which were 421 to 428 grains in the case of the 2-sigma example and 943 to 954 grains in the case of 3-sigma example. The higher values of these credible intervals were taken as the minimum sample size.

7 Testing the script for reproducibility and against other software available

To test whether the script yields reproducible results and to compare it to other software available, it was used a data set from a natural mylonitic granite sample (named MAL-05) deformed in a crustal-scale extensional shear zone, the Vivero fault (Lopez-Sanchez, 2013). The granite is a coarse-grained two-mica granite with quartz (~ 35 %), feldspar (microcline and plagioclase; ~ 60 %) and muscovite plus biotite (≤ 5 %) as main constituents. Mylonitic samples show quartz aggregates with a complete or quasi-complete dynamic recrystallization dominated by a subgrain rotation mechanism (Fig. 11) (Lopez-Sanchez, 2013). In contrast, feldspar show cataclasis with syntectonic crystallization of very fine albite-oligoclase, K-feldspar and biotite grains along fractures as well as at the feldspar rims (Lopez-Sanchez, 2013). The thin-sections were cut parallel to the mineral and stretching lineation and perpendicular to the mylonitic foliation (XZ sections). The procedure to acquire and measure the areas of the dynamically recrystallized grain sizes is summarized in Table 1.

The strategy to check reproducibility was as follows: dynamically recrystallized grain size areas were measured and their apparent diameters derived from four different locations of the same deformed sample MAL-05 (belonging to two different thin sections). Assuming that there are no differences in the dynamically recrystallized grain

SED
6, 3141–3196, 2014

size between the different locations and that the sample size obtained in each image is representative of the dynamically recrystallized grain size population, the reproducibility was tested by comparing the results obtained in each of the images measured (or a combination thereof) with the whole data set measured and observe which parameters are the most stable, and consequently reliable, to estimate the dynamically recrystallized grain size. The results obtained by the script are summarized in the Table 2 and Figs. 12 and 13.

In the number weighted approach it can be observed that the Gaussian kde peak yields lower errors compared to middle values of the modal intervals and therefore better reproducible results. It is remarkable that the maximum error obtained by the Gaussian kde peak estimator was 2.4 % with a mean of 1.3 %. On the other hand, in the area-weighted approach the area-weighted mean produces better reproducible results than the middle values of modal intervals (Table 2). In summary, the Gaussian kde peak and the area-weighted mean values produce the best reproducible results and both can be used to compare dynamically recrystallized grain sizes in dynamically recrystallized rocks. However, we think it is better to use the Gaussian kde peak estimation since it has a precise physical meaning while the mean, although has a statistical meaning, it is not clear what physically represents within the population of grains. Furthermore, and as portrayed above, the Gaussian kde peak estimators is less prone to outliers than the mean.

To test the results of the script against other software available a comparison was made with the results obtained with the *GrainSizeTools* – using the whole data set of sample MAL-05 and the Gaussian kde peak estimator – to those obtained by the software's *StripStar* (Heilbronner and Brun, 1998) and *CSDCorrections* (Higgins, 2000) (Table 3; Fig. 14). In the latter, which allows to set different shape parameters for the grains, the grains were assumed as perfect spheres and the type of measurement as the ellipse major axis, which in a sphere is equivalent to the diameter. Because these software programs were implemented to derive the actual 3-D dynamically recrystallized grain size distribution of grains from the sectional 2-D dynamically recrystallized

SED
6, 3141–3196, 2014

grain size instead of obtaining a single value, we have to set which value is adequate for comparing results. In the current case we set it to be the middle value of the modal interval of the actual (3-D) dynamically recrystallized grain size distribution. Furthermore, both software programs do not provide an automated process to estimate the number of classes (or bin size) and therefore the results can vary depending on the number of classes chosen. To overcome this problem, we used all the results obtained in a defined range of number of classes, so that the mean and other statistical parameters of interest can be calculated (Table 3). As can be seen in the Fig. 14 and Table 3, the outcomes obtained by the Gaussian kde peak are similar – within the credible intervals – to those produced by the *StripStar* and *CSDCorrections* software. In the case of the area-weighted approach, the results of the script are slightly smaller to those obtained by the *Stripstar* software using the volume weighted approach (Table 3).

As in the case of the synthetic populations with a log-normal continuous range of grain size tested, the Silverman rule multiplied by 1/3 does not yield better results. In the end, since it can be expected that deformed dynamically recrystallized rocks in nature and experiments develop continuous dynamically recrystallized grain size ranges with unimodal densities, the default rule used within the script to estimate the Gaussian kde function is the Silverman rule without any modification. In any event, this can be easily modified or new methods can be easily implemented within the script.

8 Concluding remarks and future development

The *GrainSizeTools* script provides a robust method to obtain a representative single numeric value of dynamically recrystallized grain size in dynamically recrystallized deformed rocks based on the estimation of grain sectional areas (2-D data). The script uses the Gaussian kernel density estimator peak as the best estimator, since this parameter is less prone to be shifted by the presence of outliers or multimodal distributions compared to the mean or the area-weighted mean. Furthermore, this estimator has a clear physical meaning – the most probable size of recrystallized grains – and

SED
6, 3141–3196, 2014

regardless you consider 2-D or the derived 3-D dynamically recrystallized grain size distribution yields comparable results.

The script is written in Python, a cross-platform programming language, and is free and open source. To use the script no previous knowledge of the Python language is necessary. The results are somehow similar to those obtained with the stereological software packages *StripStar* and *CSDCorrections* choosing similar statistic parameters. The main advantages of the script for paleopiezometer or paleowattometer studies are that it is specifically developed to yield a single and reproducible value from a population of apparent diameters avoiding the non-automated steps in the other implementations. This approach improves previously available methods because: (i) the bin size and the bandwidth of the Gaussian kde is based on the population features, so it prevents the user to manually choose the number of classes (or bin size/bandwidth) which penalizes the reproducibility, and (ii) it uses a continuous non-parametric density estimator – the Gaussian kernel density estimator – instead of a discrete one to find the most likely dynamically recrystallized grain size of the distribution, which improves reproducibility.

The results produced by the script are different to those obtained in the past aiming to establish a correlation between dynamically recrystallized grain size and differential stress in experiments, which mainly used logarithmic and square root grain size using 1-D methods. Therefore, the results obtained by the script requires a calibration to be used as an absolute estimator of the differential stress. For this goal it can be used as an approximation the empirical conversion matrix reported in Berger et al. (2011). Specifically, the correction factor for the area-weighted mean or the correlation factor established for the *StripStar* software in case the Gaussian kde peak value is used (see Table 5 in Berger et al., 2011). Additionally, the results of the script can be used as a relative paleopiezometer or paleowattometer by comparing the dynamically recrystallized grain size in two or more mylonite samples.

Since the widely used 1-D methods suffer from several limitations, establishing a correlation factor between different methods and statistical parameters is not an optimal

SED
6, 3141–3196, 2014

approach. The best practice in the near future would be to create a database with the dynamically recrystallized grain sizes obtained by the script in different deformed samples and minerals from different laboratory published experiments. By doing this, it will allow the calibration of the script as a reliable estimator of the absolute differential stress or rate of mechanical work.

Finally and as a cautionary note, for reproducibility issues it is crucially important that if the default parameters of the script are modified (i.e. the Fredman–Diaconis and the Silverman rules used to automatically estimate the bin size of the histogram and the bandwith of the Gaussian kde respectively), it is recommended to mention explicitly the changes made in the study as well as the version of the script thereof used. This will make possible to use the dynamically recrystallized grains of published studies in the future for comparative purposes in a reliable way. On the other hand, the methodology implemented to estimate the dynamically recrystallized grain size in this study is based on the particular features expected in highly deformed rocks recrystallized by bulging (BLG) or sub-grain rotation (SGR) recrystallization mechanisms. This means that for grain size distributions produced by other processes and involving objects geometrically more complex than near-equant objects (e.g. rocks deformed in brittle environments or dynamically recrystallized grains showing remarkably amoeboid shapes) or grain size studies that involve to derive the actual 3-D grain size distribution of grains, such as grain size distributions in non-deformed sedimentary rocks or crystal size studies of igneous rocks, the reader is referred to more complex approaches (see Higgins, 2000, 2006; Heilbronner and Barret, 2014).

Appendix A:

In the case of a perfect monodisperse population, the cross-section size probability can be directly estimated using the following equation (Sahagian and Proussevitch, 1998):

$$P(r_1 < r < r_2) = 1/R\sqrt{R^2 - r_1^2} - \sqrt{R^2 - r_2^2} \quad \text{(A1)}$$

SED
6, 3141–3196, 2014

where R is the radius of the sphere, r_1 and r_2 the lower and upper limits of the apparent section interval defined, and P the probability to cut sections within the interval defined. If we take a sphere of unit radius the equation simplifies to:

$$P(r_1 < r < r_2) = \sqrt{1 - r_1^2} - \sqrt{1 - r_2^2} \quad \text{(A2)}$$

Our aim is to find the number of grains needed to know with a certainty of 99 % that at least one of the grains measured in our data set have a size similar or with an error less than 4 % compared to the actual size. Assuming a sphere of unit radius and according to the equation shown above, we calculate for simplicity the opposite, this is, the probability that all sections obtained have a diameter shorter than 0.96 (an apparent diameter shorter or equal than 4 % with respect to the actual size) is:

$$P(0 < r < 0.96) = \sqrt{1} - \sqrt{1 - 0.96^2} = 0.72 \quad \text{(A3)}$$

If we increase the sample size (i.e. the number of random cuts), the probability that at least one random section show lengths larger than 0.96 follows the equation:

$$P_{\text{total}} = (1 - P^n) \quad \text{(A4)}$$

where n is the number of random cuts (i.e. the sample size) and P_{total} the probability that at least one apparent section is larger than 0.96 for any given n. Then we have to find when at least one of the lengths of the sections randomly cut is larger than 0.96 with a certainty of 99 %. In doing this, we find that when the sample size is 15 the P_{total} is 99.28 %. This means that when we measure just 15 grains, the chance of finding a section whose diameter has an error less than 4 % the actual size of the grains in a monodisperse system is greater than 99 %.

SED
6, 3141–3196, 2014

Appendix B: A stochastic model to simulate grain size distributions (Monte Carlo approach)

To simulate the cut-section effect, it is considered a circle of unit radius (diameter = 2) and then generates a user-defined number of random cuts (depending on the sample size desired). For this, we use a Python built-in function called *random.random* that generates a random irrational (floating point) number between 0.0 and 1.0. This represents any possible cut from the centre of the circle to its edge (Fig. B1). Then, following the Pythagorean Theorem it is calculated the length of the section (also known as chord length) using the following relationship:

$$\text{section length} = 2\sqrt{1 - d^2} \tag{B1}$$

The apparent diameters obtained can be corrected – if necessary – according to a selected diameter. The Python function implemented to simulate this effect is called *generateRandomSections* (see Supplement, *SourceCode_AnexoB.py* file). Because monodisperse systems are only affected by the cut-section effect, this Python function can be used to simulate perfect monodisperse systems. This process is repeated a number of times, as many as required to be reproducible within the level of confidence desired (see Appendix C). The data generated is stored and then plotted on a histogram (see Figs. 2, 5 and 6 within the manuscript for examples). According to the law of large numbers (or Bernoulli's law), if sample size is large enough, the Monte Carlo Simulation will produce the same results for a given accuracy obtained by the Eq. (A1) by Sahagian and Proussevitch (1998) showed in the Appendix A.

In the case of simulating a monodisperse data set with outliers (e.g. Fig. 5a and b) the procedure was as follows: first, it is established the grain size, the sample size and the ratio between the correct measures and the outliers. Once calculated the number of outliers that need to be added to the data set, the code generated a defined number of grains with a random size ranging between 1.01 to 1.5 times the recrystallized grain size defined (e.g. if the actual grain size is set to 100 microns, the outlier grains

SED
6, 3141–3196, 2014

will range between 101 to 150 microns). The maximum limit has been set arbitrarily at 1.5 times. Then, for each random grain created a random section is generated and added to the data set (see function *generateSample_withOutliers* within the *SourceCode_AnexoB.py* file in the Supplement).

To generate a data set simulating uncertainty during measurement – as in the Fig. 5c and d within the text – there are two approaches. One assumes that the uncertainty of the data is independent of the size considered and the other assumes that the error measurement is size dependent. Studies showed that the last approach is the correct one (Gualda, 2006; Berger et al., 2011). Thus, Berger et al. (2011) carried out a study involving repeated measurement on several grains and found that the error in grain size varies between 1 and 4 % for targeted grains but up to 15 % for smaller grains; this is in part due to optimizing resolution for the targeted grain sizes, resulting in considerable errors for the smallest grain sizes. Taking this into account, the procedure created to simulate such uncertainty in the data set works as follows. First, it is established the grain size, the sample size and the uncertainty expected for the sectional areas. Then it is created a number of random sections defined by the user. To generate the uncertainty within the data set: (i) it is calculated the maximum absolute error taking into account the uncertainty desired, (ii) all the values below this maximum error margin are removed to prevent negative values within the data set during the addition of random errors (there is also a practical reason for doing this since the uncertainty obtained during measurements delimits the actual optical and resolution limitations of the technique applied), and finally, (iii) a random error between zero and the maximum absolute error estimated with a random sign (i.e. positive or negative) is generated and added for each value; it is assumed that the expected error has a normal (Gaussian) distribution, this is, it is most likely that the result is closer to the actual value that the extreme values defined (see function *generateSample_withUncertainty* within the *SourceCode_AnexoB.py* file in the Supplement).

To simulate the intersection probability effect in case of polydisperse populations, first we create a large population of grains (say a million) with a defined distribution and

SED
6, 3141–3196, 2014

then calculate the individual volumes of each grain and the total volume. At that point, assuming that the probability of intersecting a particular grain is directly proportional to its volume respect to total volume, we normalize the individual volumes of the grains respect to the total volume. Finally, we create an array of data with the cumulative sum of the elements. As an example, imagine a list of three grains with diameters 2, 3 and 5 (i.e. [2, 3, 5]). If we calculate the volume ([0.52, 4.19, 14.14]) and then normalize it to the total volume (18.85) we obtain the following array values [0.028, 0.222, 0.750]. Finally, we generate a cumulative sum of elements [0.028, 0.25, 1.0]. Once this array is created a desired number of random values between 0.0 and 1.0 are generated. Each value obtained is used to find which grain is going to be sectioned according to their probability (i.e. volume) using the list of cumulative sum of elements created. Returning to our example, if we obtain as a random value 0.21, we find the position in the cumulative list that meets the following criteria value > 0.21. In this case it is the number in the second position in the list, therefore the grain to pick up and sectioned from the original list of grain sizes is the grain located in the second position which has a diameter of 3. This was repeated 5000 times to create a large population of grains affected by the intersection probability and, later, by the cut-section effect from our original population of one million grains. Due to the notable differences between the original population (10^6) and the new one (5000) it is considered highly unlikely ($\ll 0.05$) that in the process of simulating the intersection probability effect the same grain is chosen twice.

To simulate a bimodal discrete distribution (Fig. 5), we implement a Python function called *generatebimodalSample*. This function first generates two populations of grains with different sizes and in a proportion defined by the user. The function takes into account the probability section and the cut-section effects to generate the population of apparent diameters of the grains. The *generatebimodalSample* requires that the user introduces the following parameters: (i) the grain size of the population A, (ii) the grain size of the population B, (iii) the sample size and (iv) the ratio between the two populations (e.g. if ratio = 0.8, it means that population A represents 80 % – in number

SED
6, 3141–3196, 2014

– of the total population). The function returns a text file with the random apparent diameters (2-D) generated.

To produce a log-normal distribution of spheres we implemented a Python function called *generateLogNormSample*. This function first creates a log-normal population using the built-in function *scipy.stats.lognorm.rvs* from the *scipy.stats module*, then selects a subpopulation of size 5000 affected by the intersection probability effect and finally converts the actual population in a population of apparent diameters (2-D). The *generateLogNormSample* function requires that the user introduces the following parameters: (i) grain size, (ii) sample size and (iii) shape and scale parameters of the log-normal distribution. The function returns a text file with the random apparent diameters (2-D) population and a plot showing the distribution of the actual 3-D population as a histogram and a probability density function.

The code implemented to perform this task is shown in the Supplement file *SourceCode_AnexoB.py*.

Appendix C: A stochastic model to find the minimum number of grains necessary to achieve reproducibility (Monte Carlo approach)

The simulation operates as follows:

1. A representative number of samples (say 2×10^5 or more) of a given size is created. Usually begins with a sample size as little as possible, this is, of size one. For each sample created the average grain size is calculated and stored.

2. To test the reproducibility, the mean and the SD of the data set for the current sample is calculated (i.e. the mean value and the SD of the average grain sizes obtained for each sample created).

3. In order to compare samples with different mean values, it is necessary to view the SD in the context of the mean. Hence, to normalize the data obtained, it

SED
6, 3141–3196, 2014

is calculated a modified version of the coefficient of variation (originally the SD divided by the mean; σ/μ). We use the sigma-2 and sigma-3 values instead of the SD (sigma-1). Based on the study of Berger et al. (2011), the errors in the diameter measurements are up to 4 % for targeted grains. Therefore, the modified coefficient of variation has to meet the following condition:

$$2\sigma/\text{mean or } 3\sigma/\text{mean} < 0.04 \quad \text{(C1)}$$

If the condition is not satisfied, the sample size is increased (with a step size defined by the user) and the process initiates once again until the condition is satisfied.

4. When the condition is satisfied, the sample size for the defined condition is reported and a number of plots showing the evolution of the mean, the SD and the modified coefficient of variation throughout the process of increasing the sample size are generated.

   The code implemented to perform this task is shown in the attached file: *findSampleSize.py*

The Supplement related to this article is available online at doi:10.5194/sed-6-3141-2014-supplement.

Author contributions. Marco A. Lopez-Sanchez designed the simulations, developed the Python code, interpreted the data and drafted the manuscript. Sergio Llana-Fúnez contributed with new ideas and tested the scripts independently during the preparation of the manuscript.

Acknowledgements. The study of the dynamically recrystallized grain size distribution in dynamically recrystallized rocks was undertaken during the last stages of the Ph.D. of the author and funded by research grant CGL2010-14890 from the Spanish Government and a Severo Ochoa doctoral fellowship (BP07-120) from the Principality of Asturias Government (Spain).

SED
6, 3141–3196, 2014

References

Abrams, H.: Grain size measurement by the intercept method, Metallography, 4, 59–78, doi:10.1016/0026-0800(71)90005-X, 1971.

Austin, N. J. and Evans, B.: Paleowattmeters: a scaling relation for dynamically recrystallized grain size, Geology, 35, 343–346, doi:10.1130/G23244A.1, 2007.

Barnhoorn, A., Bystricky, M., Burlini, L., and Kunze, K.: The role of recrystallisation on the deformation behaviour of calcite rocks: large strain torsion experiments on Carrara marble, J. Struct. Geol., 26, 885–903, doi:10.1016/j.jsg.2003.11.024, 2004.

Bashtannyk, D. M. and Hyndman, R. J.: Bandwidth selection for kernel conditional density estimation, Comput. Stat. Data An., 36, 279–298, doi:10.1016/S0167-9473(00)00046-3, 2001.

Berger, A., Herwegh, M., Schwarz, J. O., and Putlitz, B.: Quantitative analysis of crystal/grain sizes and their distributions in 2-D and 3-D, J. Struct. Geol., 33, 1751–1763, doi:10.1016/j.jsg.2011.07.002, 2011.

De Bresser, J. H. P., Ter Heege, J. H., and Spiers, C. J.: Grain size reduction by dynamic recrystallization: can it result in major rheological weakening?, Int. J. Earth Sci., 90, 28–45, doi:10.1007/s005310000149, 2001.

Emmermann, R. and Lauterjung, J.: The German Continental Deep Drilling Program KTB: overview and major results, J. Geophys. Res., 10, 18179–18201, doi:10.1029/96JB03945, 1997.

Freedman, D. and Diaconis, P.: On the histogram as a density estimator: L2 theory, Z. Wahrscheinlichkeit., 57, 453–476, doi:10.1007/BF01025868, 1981.

Guillopé, M. and Poirier, J. P.: Dynamic re-crystallization during creep of single-crystalline halite: an experimental study, J. Geophys. Res., 84, 5557–5567, doi:10.1029/JB084iB10p05557, 1979.

Gualda, G.: Crystal size distributions derived from 3-D data sets: sample size versus uncertainties, J. Petrol., 47, 1245–1254, doi:10.1093/petrology/egl010, 2006.

Heilbronner, R.: Automatic grain boundary detection and grain size analysis using polarization micrographs or orientation images, J. Struct. Geol., 22, 969–981, doi:10.1016/S0191-8141(00)00014-6, 2000.

Heilbronner, R. and Barret, S. (Eds.): Image Analysis in Earth Sciences, Springer-Verlag, Berlin, 2014.

SED
6, 3141–3196, 2014

Heilbronner, R. and Bruhn, D.: The influence of three-dimensional grain size distributions on the rheology of polyphase rocks, J. Struct. Geol., 20, 695–705, doi:10.1016/S0191-8141(98)00010-8, 1998.
Heilbronner, R. and Tullis, J.: Evolution of c axis pole figures and grain size during dynamic recrystallization: results from experimentally sheared quartzite, J. Geophys. Res., 111, B10202, doi:10.1029/2005JB004194, 2006.
Herwegh, M.: A new technique to automatically quantify microstructures of fine grained carbonate mylonites: two-step etching combined with SEM imaging and image analysis, J. Struct. Geol., 22, 391–400, doi:10.1016/S0191-8141(99)00165-0, 2000.
Herwegh, M., de Bresser, J., and ter Heege, J.: Combining natural microstructures with composite flow laws: an improved approach for the extrapolation of lab data to nature, J. Struct. Geol., 27, 503–521, doi:10.1016/j.jsg.2004.10.010, 2005.
Higgins, M. D.: Measurement of crystal size distributions, Am. Mineral., 85, 1105–1116, 2000.
Higgins, M. D. (Ed.): Quantitative Textural Measurements in Igneous and Metamorphic Petrology, Cambridge University Press, Cambridge, 2006.
Hunter, J. D.: Matplotlib: a 2-D graphics environment, Comput. Sci. Eng., 9, 90–95, doi:10.1109/MCSE.2007.55, 2007.
Karato, S. I., Toriumi, M., and Fujii, T.: Dynamic recrystallization of olivine single crystals during high-temperature creep, Geophys. Res. Lett., 7, 649–652, doi:10.1029/GL007i009p00649, 1980.
Knipe, R. J. and Law, R. D.: The influence of crystallographic orientation and grain boundary migration on microstructural and textural evolution in a SC mylonite, Tectonophysics, 135, 155–169, doi:10.1016/0040-1951(87)90158-2, 1987.
Kozlovsky, Y. A. (Ed.): The Superdeep Well of the Kola Peninsula, Springer Verlag, Berlin, 1987.
Limpert, E., Stahel, W. A., and Abbt, M.: Log-normal distributions across the sciences: keys and clues, BioScience, 51, 341–352, doi:10.1641/0006-3568(2001)051[0341:LNDATS]2.0.CO;2, 2001.
Lopez-Sanchez, M. A.: Análisis tectónico de la Falla de Vivero (Galicia, NO de España), Ph.D. thesis, Universidad de Oviedo, 2013.
Lutton, M. J. and Sellars, C. M.: Dynamic recrystallization in nickel and nickel-iron alloys during high temperature deformation, Acta Metall. Mater., 17, 1033–1043, doi:10.1016/0001-6160(69)90049-2, 1969.

SED
6, 3141–3196, 2014

Mancktelow, N. S.: Quartz textures form the Simplon Fault Zone, southwest Switzerland and north Italy, Tectonophysics, 135, 133–153, doi:10.1016/0040-1951(87)90157-0, 1987.
Means, W. D.: Microstructure and micromotion in recrystallization flow of octachloropropane: a first look, Geol. Rundsch., 72, 511–528, doi:10.1007/BF01822080, 1983.
Mercier, J.-C. C., Anderson, D. A., and Carter, N. L.: Stress in the lithosphere: inferences from steady state flow of rocks, Pure Appl. Geophys., 115, 199–226, doi:10.1007/BF01637104, 1977.
Michibayashi, K.: Syntectonic development of a strain-independent steady-state grain size during mylonitization, Tectonophysics, 222, 151–154 doi:10.1016/0040-1951(93)90046-M, 1993.
Nicolas, A. and Poirier, J. P.: Crystalline Plasticity and Solid State Flow in Metamorphic Rocks, Wiley Interscience, London, 1976.
Oliphant, T. E.: Python for scientific computing, Comput. Sci. Eng., 9, 10–20, doi:10.1109/MCSE.2007.58, 2007.
Pieri, M., Burlini, L., Kunze, K., Stretton, I., and Olgaard, D. L.: Rheological and microstructural evolution of Carrara marble with high shear strain: results from high temperature torsion experiments, J. Struct. Geol., 23, 1393–1413, doi:10.1016/S0191-8141(01)00006-2, 2001.
Platt, J. P. and Behr, W. M.: Grainsize evolution in ductile shear zones: implications for strain localization and the strength of the lithosphere, J. Struct. Geol., 33, 537–550, doi:10.1016/j.jsg.2011.01.018, 2011.
Poirier, J. P. and Guillopé, M.: Deformation induced recrystallization of minerals, B. Mineral., 102, 67–74, 1979.
Poirier, J. P. and Nicolas, A.: Deformation-induced recrystallization due to progressive misorientation of subgrains, with special reference to mantle peridotites, J. Geol., 83, 707–720, 1975.
Post, A. and Tullis, J.: A recrystallized grain size piezometer for experimentally deformed feldspar aggregates, Tectonophysics, 303, 159–173, doi:10.1016/S0040-1951(98)00260-1, 1999.
Ranalli, G.: Grain size distribution and flow stress in tectonites, J. Struct. Geol., 6, 443–447, doi:10.1016/0191-8141(84)90046-4, 1984.
Ross, J. V., Ave Lallemant, H. G., and Carter, N. L.: Stress dependence of recrystallized grain and subgrain size in olivine, Tectonophysics, 70, 39–61, doi:10.1016/0040-1951(80)90020-7, 1980.

SED
6, 3141–3196, 2014

Royet, J.-P.: Stereology: a method for analysing images, Prog. Neurobiol., 37, 433–474, doi:10.1016/0301-0082(91)90009-P, 1991.
Rutter, E. H.: Experimental study of the influence of stress, temperature, and strain on the dynamic recrystallization of Carrara marble, J. Geophys. Res., 100, 24651, doi:10.1029/95JB02500, 1995.
Sahagian, D. L., Proussevitch, A. A.: 3-D particle size distributions from 2-D observations: stereology for natural applications, J. Volcanol. Geoth. Res., 84, 173–196, doi:10.1029/95JB02500, 1998.
Schmid, S. M.: Textures of geological materials: computer model predictions vs. empirical interpretations based on rock deformation experiments and field studies, in: Textures of Geological Materials, DGM Informationsgesellschaft Verlag, Uberursel, Germany, 279–301, 1994.
Schmid, S. M., Paterson, M., and Boland, J.: High temperature flow and dynamic recrystallization in carrara marble, Tectonophysics, 65, 245–280, doi:10.1016/0040-1951(87)90157-0, 1980.
Schneider, C. A., Rasband, W. S., and Eliceiri, K. W.: NIH Image to ImageJ: 25 years of image analysis, Nat. Methods, 9, 671–675, doi:10.1038/nmeth.2089, 2012.
Scott, D. W.: On optimal and data-based histograms, Biometrika, 66, 605–610, doi:10.1093/biomet/66.3.605, 1979.
Scott, D. W.: Multivariate Density Estimation: Theory, Practice, and Visualization, John Wiley & Sons, New York, Chicester, 1992.
Shimizu, I.: Theories and applicability of grain size piezometers: the role of dynamic recrystallization mechanisms, J. Struct. Geol., 30, 899–917, doi:10.1016/j.jsg.2008.03.004, 2008.
Silverman, B. W.: Density estimation for statistics and data analysis, in: Monographs on Statistics and Applied Probability, Chapman and Hall, London, 1986.
Stipp, M. and Tullis, J.: The recrystallized grain size piezometer for quartz, Geophys. Res. Lett., 30, 2088, doi:10.1029/2003GL018444, 2003.
Stipp, M., Stünitz, H., Heilbronner, R., and Schmid, S. M.: The eastern Tonale fault zone: a "natural laboratory" for crystal plastic deformation of quartz over a temperature range from 250 to 700 °C, J. Struct. Geol., 24, 1861–1884, doi:10.1016/S0191-8141(02)00035-4, 2002.
Stipp, M., Tullis, J., and Behrens, H.: Effect of water on the dislocation creep microstructure and flow stress of quartz and implications for the recrystallized grain size piezometer, J. Geophys. Res., 111, B04201, doi:10.1029/2005JB003852, 2006.

SED
6, 3141–3196, 2014

Stipp, M., Tullis, J., Scherwath, M., and Behrmann, J.: A new perspective on paleopiezometry: dynamically recrystallized grain size distributions indicate mechanism changes, Geology, 38, 759–762, doi:10.1130/G31162.1, 2010.

Stünitz, H.: Syndeformational recrystallization – dynamic or compositionally induced?, Contrib. Mineral. Petr., 131, 219–136, doi:10.1007/s004100050390, 1998.

Turlach, B. A.: Bandwidth selection in kernel density estimation: a review, Institut für Statistik und Ökonometrie, Humboldt-Universität zu Berlin, Berlin, 1993.

Twiss, R. J.: Theory and applicability of a recrystallized grain size paleopiezometer, Pure Appl. Geophys., 115, 227–244, doi:10.1007/BF01637105, 1977.

Urai, J. L., Means, W. D., and Lister, G. S.: Dynamic recrystallization of minerals, in: Mineral and Rock Deformation: Laboratory Studies – the Paterson Volume, edited by: Hobbs, B. E. and Heard H. C., Am. Geophys. Union Geophysical Monograph 36, Washington DC, 161–199, 1986.

SED
6, 3141–3196, 2014

Table 1. Steps for obtaining the cross-sectional areas of the grains using the *ImageJ* software.

1. We acquire several light microscopy digital images from four different areas of the thin section using cross polarized light with or without the gypsum plate inserted. In two of the areas chosen, four different images were taken at the same location, a pair of cross polarized and cross polarized with the gypsum plate inserted and other similar pair but rotated 45°. Then the images were superimposed. This allows to use any of the acquired images in case grain boundaries appear fuzzy in one or more of the input images. The images in the four different areas were taken with different resolutions for comparison, varying from 0.72 micron pixel^{-1} to 0.35 micron pixel^{-1}.
2. Digital image processing to enhance grain boundaries (basically set a correct contrast/brightness ratio and apply a high-pass filter to enhance boundaries if necessary).
3. Manual outlining of the quartz grains using a vector-graphics application. Each grain is converted into a closed polygon filled with black color and making the boundary lines white. In this step grains not considered dynamically recrystallized or cut by the image margins were discarded.
4. A grey-scale raster image with the same resolution of the original image is created. We ensure that the grain boundaries have a width of two/three pixels. This will be used later to correct the diameters obtained from the areas taking into account the resolution of the digital images.
5. Measurement of cross-sectional areas using the image analysis software *ImageJ*. Basically, the steps are as follows: (i) convert the image into an 8 bit binary image; (ii) set the scale of the image; (iii) set the type of measure/s to be done, these includes the area and other parameters of interest; and (iv) measure the area of each grains individually using "Analyze particles".
6. The cross-sectional areas obtained are saved as text file to analyze the data later using the *GrainSizeTools* script.

SED
6, 3141–3196, 2014

Table 2. Results for different parameters using different sub-data sets from sample MAL-05.

Data sets	Number weighted approach						Area-weighted approach					
	Gaussian kde peak	Error (%)[a]	Middle value of modal interval Scott rule[b]	Error (%)[a]	Middle value of modal interval F–D rule[c]	Error (%)[a]	Middle value of modal interval Scott rule[b]	Error (%)[a]	Middle value of modal interval F–D rule[c]	Error (%)[a]	Area-weighted mean value	Error (%)[a]
sample 01	34.3	2.4	30.6	5.1	36.8	9.4	51.0	3.1	51.5	10.9	57.4	0.7
sample 02	33.3	0.6	31.1	3.6	33.8	0.6	44.9	9.2	49.4	6.5	57.3	0.5
sample 03	34.2	2.1	31.5	2.3	38.5	14.4	52.5	6.2	50.4	8.5	58.3	2.3
sample 04	33.9	1.2	34.7	7.4	31.9	5.2	47.3	4.4	46.6	0.3	54.8	3.9
ref. 01–02	33.5	0.0	35.1	8.8	34.0	1.2	45.9	7.2	50.0	7.8	57.3	0.5
ref. 03–04	34.0	1.5	34.5	6.8	34.9	3.7	50.4	1.8	51.3	10.5	56.6	0.7
means		**1.3**		**5.7**		**5.8**		**5.3**		**7.4**		**1.4**
all data	**33.5**		**32.3**		**33.6**		**49.5**		**46.4**		**57.0**	

[a] Relative errors taking as reference the result using the whole data set.
[b] Values obtained using the Scott rule (Scott, 1979) to estimate the bin size of the histogram and bar plots.
[c] Values obtained using the Freedman–Diaconis rule (Freedman and Diaconis, 1981) to estimate the bin size of the histogram and bar plots.

SED
6, 3141–3196, 2014

Table 3. Results producing by the different script/software's considered using the whole dataset of sample MAL-05.

Software/Script	Best estimation	Standard dev.	Credible intervals[d]	Range	Best estimation (area/volume weighted)
GrainSizeTools[a]	**33.5**				**46.4**
StripStar[b]	**33.4**	2.82	**31.4–35.4**	29.6–39.5	53.5 (**51.6–55.4**)[d]
CSD corrections[c]	**34.3**	2.39	**33.0–35.7**	31.6–38.5	

[a] Best estimation based on Gaussian kde's peak (number weighted) and the middle of the modal interval (area-weighted).
[b] Best estimation based on the mean of the middle of the modal intervals considering different number of classes (between 10 and 20).
[c] Best estimation based on the mean of the middle of the modal intervals considering different number of classes (between 5 and 20).
[d] Bayesian credibility interval (i.e. there is a 95 % probability that the true value falls within the credible region).

SED
6, 3141–3196, 2014

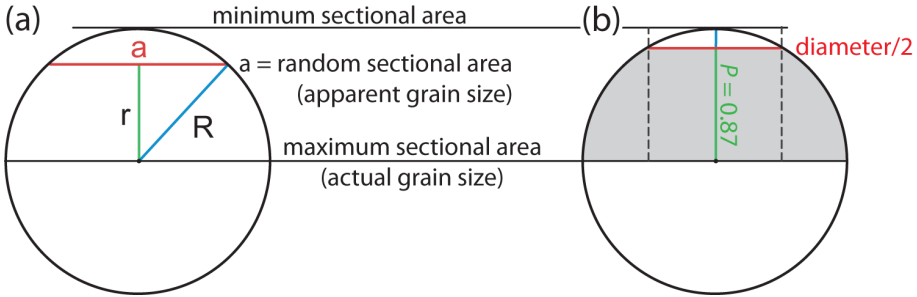

Figure 1. (a) Possible sections through a circle (sphere projection). *R* is the radius, *a* the section or chord length of a random section and *r* the apothem, this is, the distance from the centre of the circle to the midpoint of the section length. The chord length correspond with the apparent diameter and ranges between zero and the actual diameter of the grain when the section cuts through the centre of the circle. **(b)** Example showing an apparent section that correspond with the half of the actual diameter. The scheme allows to visualize that to obtain apparent diameters larger than the half of the actual diameter is most likely (P = 0.87) than the opposite.

SED
6, 3141–3196, 2014

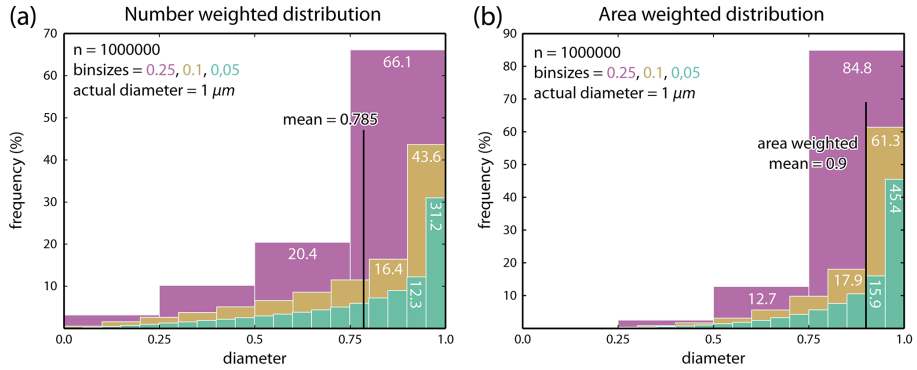

Figure 2. Grain size distribution plots producing by cutting a sphere of the same size randomly (monodisperse system). **(a)** Histogram of apparent diameters from a population of spheres of size 1 showing different number of classes or bin sizes. The actual diameter of the grain is always within the most frequent class of the histogram, the modal interval. Specifically in the upper limit of the same. The mean of the population is always 0.785 times the actual grain size for a representative sample size. **(b)** Same population as **(a)** but a bar plot showing the area percentages of equivalent diameters (i.e. the sum of the areas of the grains respect to the total for each grain size interval defined). The area-weighted mean of the population is 0.9 times the actual grain size for a representative sample size.

SED
6, 3141–3196, 2014

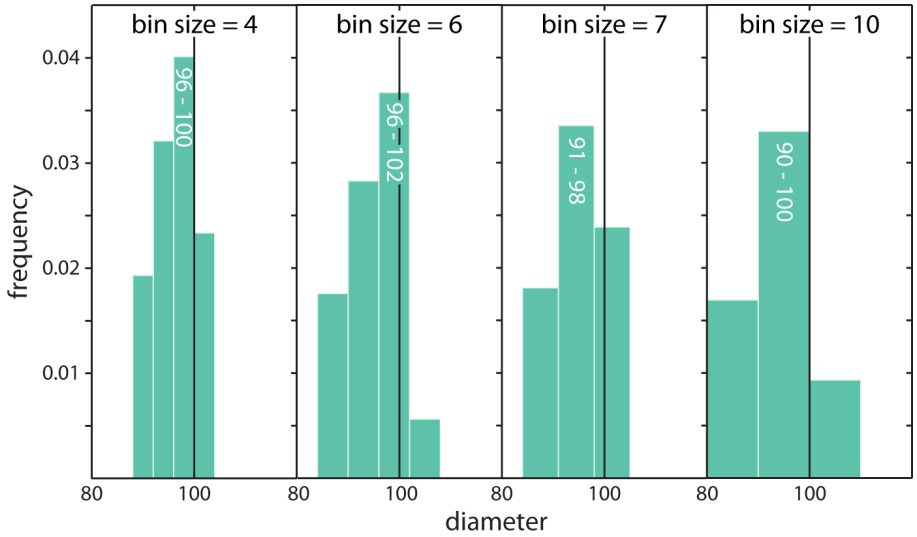

Figure 3. Plots showing the effect of choosing different bin sizes for the same data set. The monodisperse data set is formed by 5997 measures, the actual grain size was set in 100 and the absolute maximum uncertainty in measure within the data was set in ±4 (4 % of the actual size). For clarity, only the bins surrounding the actual grain size are showed. Because 4 and 10 are perfect multiples of 100, the upper limit of the modal interval coincides with the actual grain size. In this example, 4 is the best bin size since we know that the uncertainty within the data is the 0.04. Bin sizes higher than 4 do not produce best estimations and instead produces worse precision (i.e. wide intervals). In the case that the bin size is not a multiple of the actual grain size – the most probable scenario since we unknown the value we are looking for – the actual value may or may not be within the modal interval, although always close.

SED
6, 3141–3196, 2014

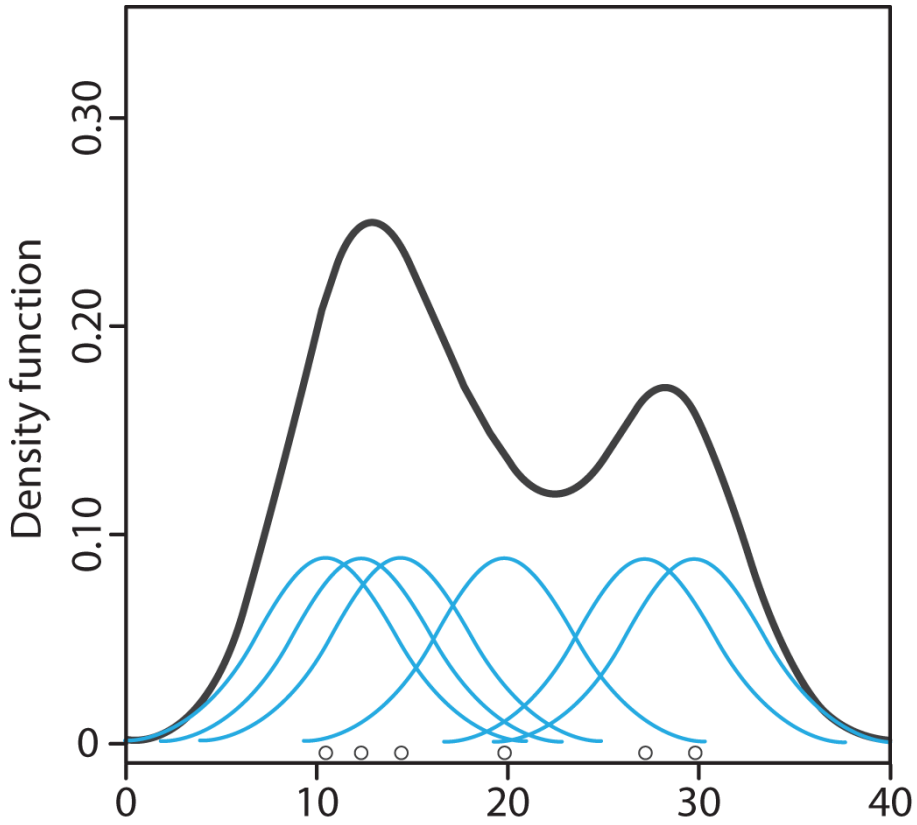

Figure 4. The Gaussian kernel density estimator is a function that stacks a Gaussian "bell curve" on top of each measurement and whose SD, determined by the local probability density, defines the bandwidth (the equivalent to the histogram's bin size/width). This function is a non-parametric density estimator that, contrary to the histogram, is smooth and independent of end points.

SED
6, 3141–3196, 2014

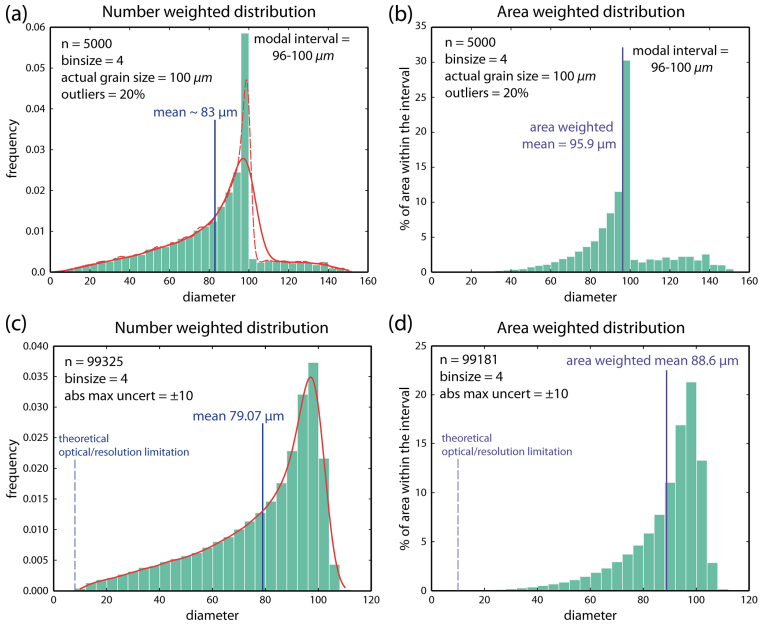

Figure 5. (a, b) Number and area-weighted plots showing the distribution of apparent diameters of a population of spheres of size 100 in which the 20 % of the data are outliers (not fully recrystallized grains; see Appendix B for details). **(c, d)** Number and area-weighted plots showing the distribution of apparent diameters of a population of spheres of size 100 with uncertainty in the measure. The maximum uncertainty during the outline of the grains was set in ±10 (10 % the actual size). This uncertainty limit also established a theoretical optical/resolution limitation of the measure (i.e. simulates that the technique does not allow grain measuring below the established limit). The distribution of apparent diameters no longer has an ideal *J-shaped* and there are apparent diameters above the actual value. The number weighted plots also shown the Gaussian kernel density estimator using the Silverman rule (continuous red line) and the Silverman rule multiplied by 1/3 (dashed red line) to estimate the bandwidth.

SED
6, 3141–3196, 2014

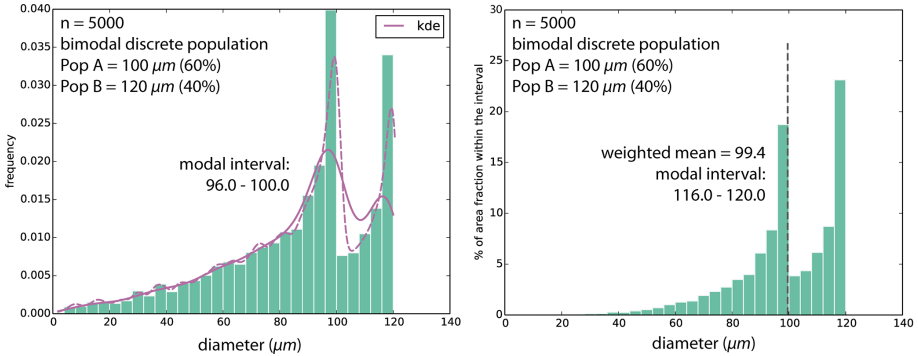

Figure 6. Grain size distribution plots of a bimodal discrete population consisting of a 60/40 % mixture of spherical particles with sizes 100 and 120 respectively. The contribution in volume is 46.5/53.5 % respectively. The two local maxima in both plots indicate the existence of two population of spheres with sizes specified by the local maxima's. Both plots show different modal intervals due to the different approach. The area-weighted plot locate the modal interval in the population that represents the major/main phase (i.e. the volumetric contribution). The number weighted plot shown the Gaussian kernel density estimator using the Silverman rule (continuous purple line) and the Silverman rule multiplied by 1/3 (dashed purple line) to estimate the bandwidth.

SED
6, 3141–3196, 2014

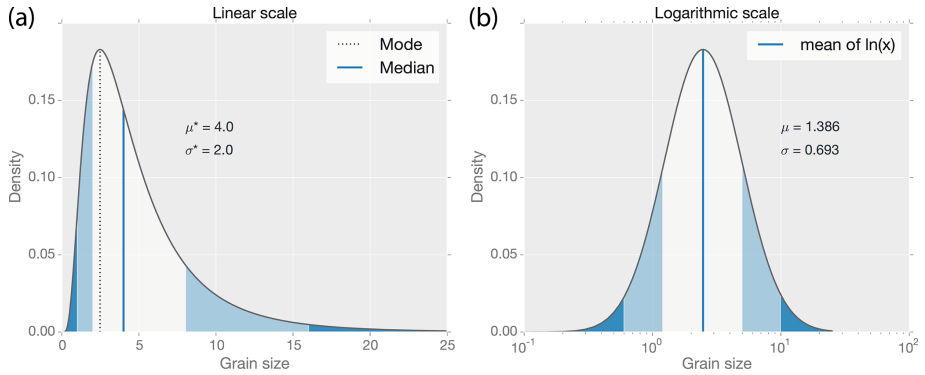

Figure 7. A log-normal distribution with original linear scale **(a)** and with logarithmic scale **(b)**. Areas under the curve correspond to one and two SD ranges of the normal distribution. μ * value is the median or geometric mean, called the "scale" parameter, while σ* value is the multiplicative SD, called the "shape" parameter. Both, μ^* and σ^*, are the "back-transformed" values of mean (μ) and SD (σ) of the log(x) distribution.

SED
6, 3141–3196, 2014

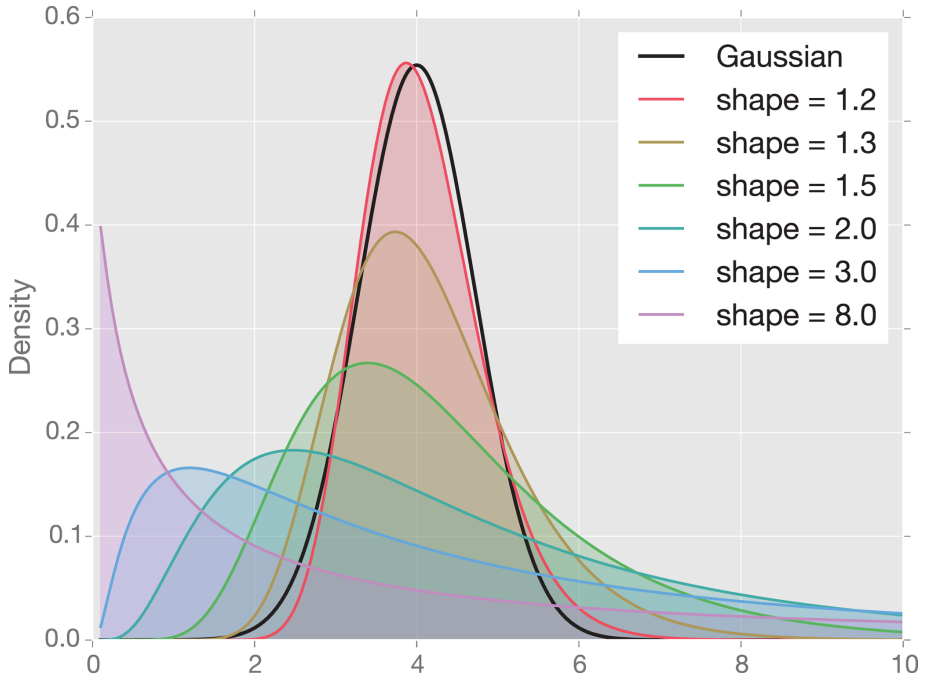

Figure 8. Probability density functions of selected log-normal distributions with different shape values (σ^*) but same scale ($\mu^* = 4$) compared with a normal or Gaussian distribution (black). A change in μ^* affects the scaling in horizontal and vertical directions, but the essential shape σ^* remains the same. Note that for a same scale parameter the theoretical range of the grain size expected is different considering different shape parameters. Based on Fig. 4 in Limpert et al. (2001).

SED
6, 3141–3196, 2014

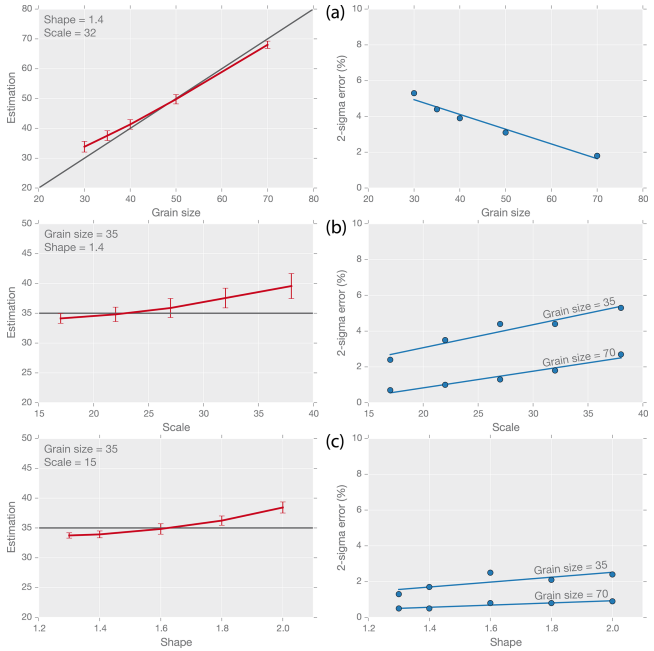

Figure 9. Results of the Gaussian kde peak estimator in the performed log-normal simulations. Each synthetic sample of apparent diameters have a sample size of 12 500 grains and the cut-section and intersection probability effects were taken into account. One hundred trials for each defined log-normal population of grains was performed. **(a)** Estimations using the grain size as variable and values of shape and scale fixed at 1.4 and 32 respectively. On the left, the results of the estimation (in red) respect to the expected (in black). Error bars correspond to the absolute 2-sigma error obtained. On the right, the relative 2-sigma errors respect to the mean (in blue). **(b)** Estimations using the scale parameter as variable and the grain size and the shape fixed at 35 and 1.4 respectively. On the left it is shown also the relative 2-sigma error considering the grain size as 70. **(c)** Estimations using the shape parameter as variable and the grain size and the scale fixed at 35 and 15 respectively.

SED
6, 3141–3196, 2014

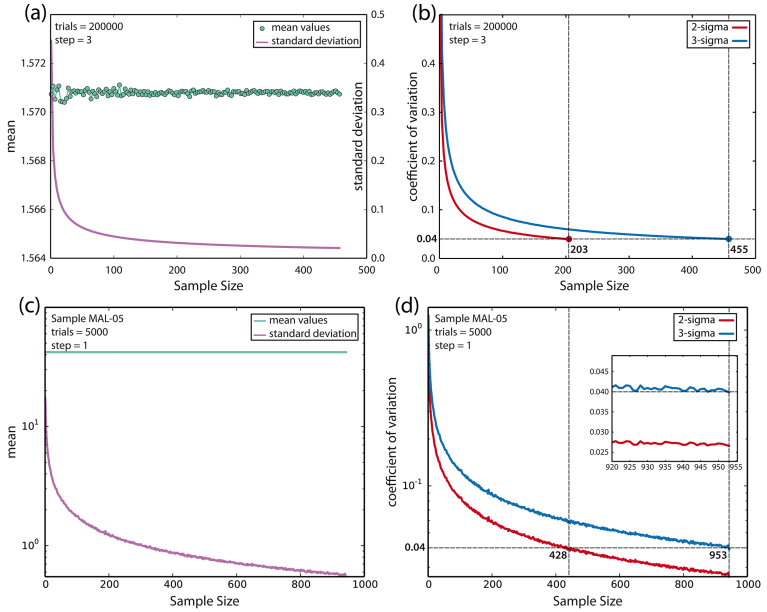

Figure 10. Results of the Monte Carlo simulations to find how many grains are needed to achieve reproducibility using a synthetic monodisperse population of apparent diameters **(a, b)** and a natural dynamically recrystallized mylonite **(c, d)**. **(a)** Evolution of the mean and the SD during the increasing of sample size. Note that the mean barely changes its value due to the large number of trials used in each sample size while the SD declined monotonically as we increased the number of samples. **(b)** Evolution of the coefficient of variation (σ/mean), using the sigma-2 and sigma-3 values during the increasing of sample size. The plot shows that when we measure 203 (for 2-sigma) or 455 (for 3-sigma) grains the variation of grain size estimations in each trial is less than 4 %, this is, less than the typical error found when repeating measurements of the same grain (Berger et al., 2011). **(c, d)** Same as above but using bootstrapping with a data set belonging to a natural mylonite (MAL-05). Note that for clarity the vertical axis have a logarithmic scale. The inset in **(d)** show a linear scale.

SED
6, 3141–3196, 2014

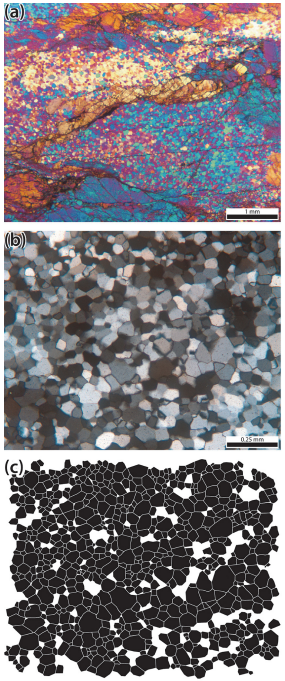

Figure 11. Quartz microstructure in sample MAL-05. **(a)** General aspect of Penedo Gordo mylonites under optical microscope (crossed polars, gypsum plate inserted). Note that original quartz grains are almost fully recrystallized and have a strong lattice preferred orientation. **(b)** Optical micrograph (crossed polars) showing the typical aspect of dynamically recrystallized quartz grains. **(c)** Quartz grain boundaries from micrograph **(b)**. This is the data set 02 in Fig. 13.

SED
6, 3141–3196, 2014

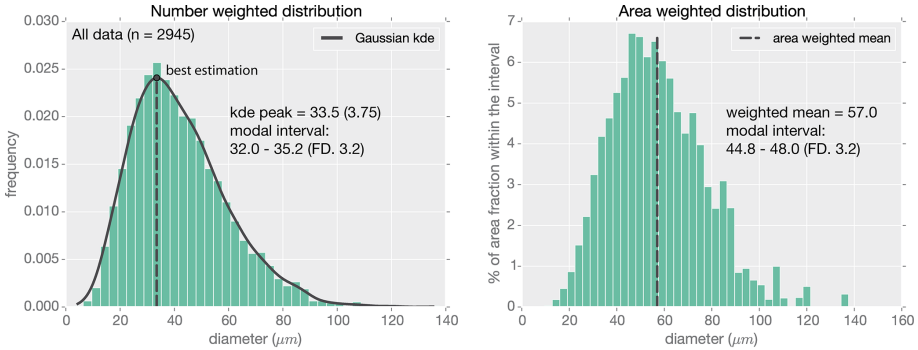

Figure 12. *GrainSizeTools* script results using the full data set from the natural sample MAL-05. The best estimation is 33.5 microns.

SED
6, 3141–3196, 2014

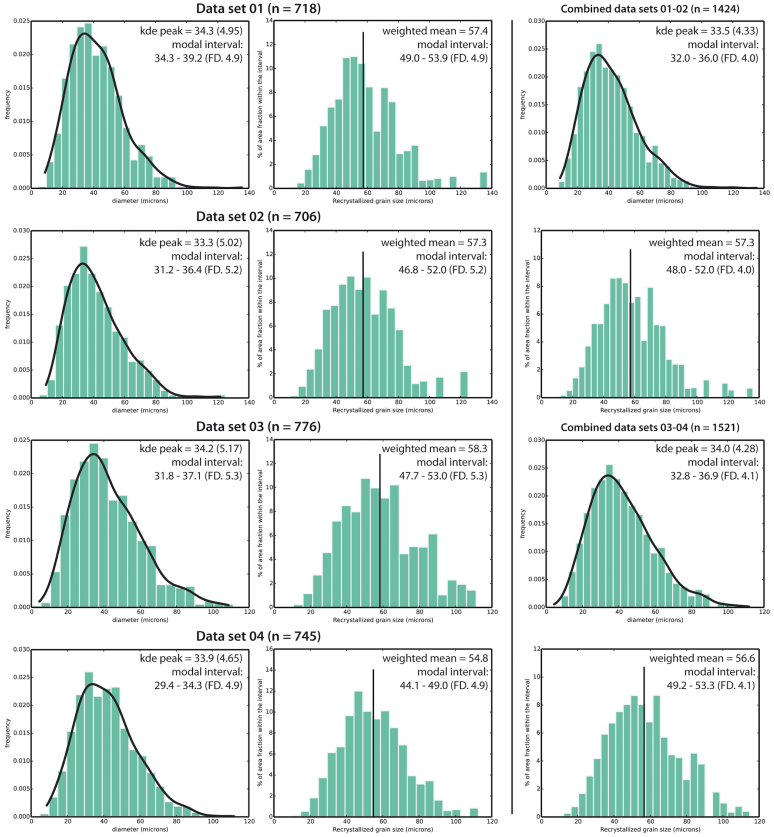

Figure 13. *GrainSizeTools* script results using different sub-data sets from the natural sample MAL-05 to test reproducibility.

SED
6, 3141–3196, 2014

GrainSizeTools: a Python script

M. A. Lopez-Sanchez and S. Llana-Fúnez

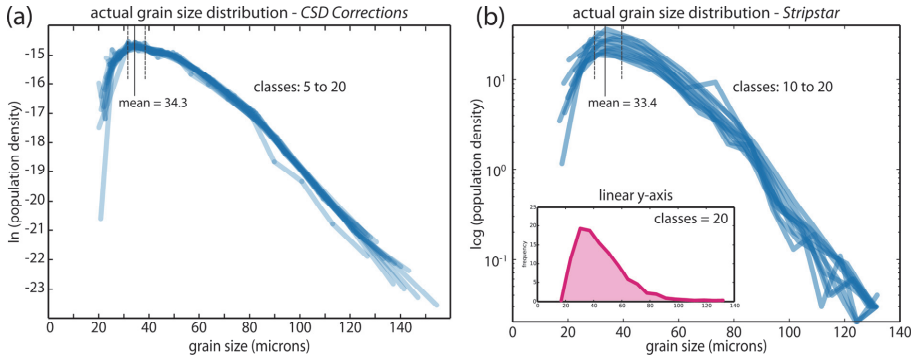

Figure 14. Estimated actual (3-D) grain size distribution from sample MAL-05 performed with *CSD Corrections* **(a)** and *Stripstar* **(b)** software's. To draw the lines, it was joined the middle values of each bin estimated by the software's taking into account different number of classes. The modal grain size and other statistical parameters of interest were calculated using all the middle values of the modal intervals obtained. The inset in **(b)** is the curve estimated by the *StripStar* software considering 20 classes but using a linear scale instead of logarithmic in the vertical axis. Note that the actual (3-D) grain size curve seem to be similar to a log-normal grain size distribution.

SED
6, 3141–3196, 2014

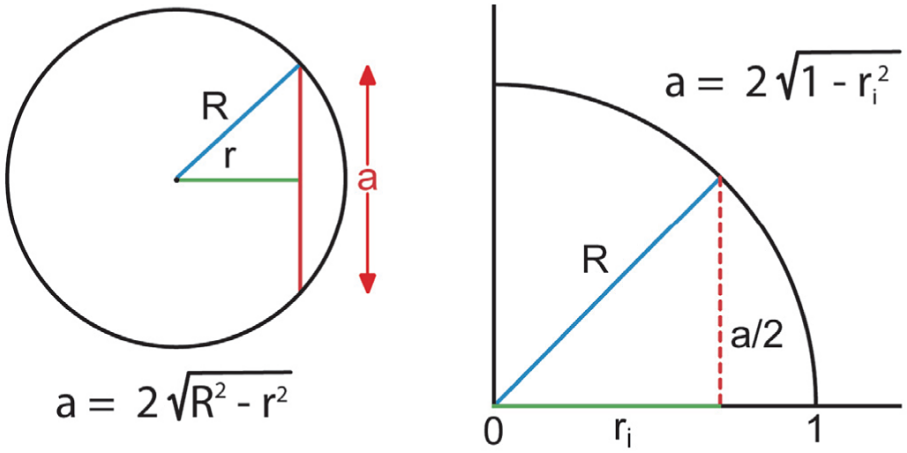

Figure B1. Model to generate apparent random sections through a sphere and calculate the apparent diameter. Following the Pythagorean Theorem, to calculate the chord or section length through a sphere we need to know the radius (R) and the apothem (r). Taking a sphere of radius 1, we generate random apothems (r_i) between 0 and 1 and then calculates and store the apparent diameters (from 2 to 0).

SED
6, 3141–3196, 2014